Dexras1 Induces Dysdifferentiation of Oligodendrocytes by Inhibiting the cAMP-CREB Pathway in White Matter Injury After Subarachnoid Hemorrhage

Yuanjun Xin
Chongqing University of Medical Science Clinical College: The First Affiliated Hospital of Chongqing Medical University

Hongxia Zhang
Chongqing University of Medical Science Clinical College: The First Affiliated Hospital of Chongqing Medical University

Jie Chen
Chongqing University of Medical Science: Chongqing Medical University

Yidan Liang
Chongqing University of Medical Science Clinical College: The First Affiliated Hospital of Chongqing Medical University

Jun Zhao
Chongqing University of Medical Science Clinical College: The First Affiliated Hospital of Chongqing Medical University

Xiang Xiang
Chongqing University of Medical Science Clinical College: The First Affiliated Hospital of Chongqing Medical University

Fu Ming Liang
Chongqing University of Medical Science Clinical College: The First Affiliated Hospital of Chongqing Medical University

Wenqiao Fu
Chongqing University of Medical Science Clinical College: The First Affiliated Hospital of Chongqing Medical University

Hao Huang
Chongqing University of Medical Science Clinical College: The First Affiliated Hospital of Chongqing Medical University

Xintong Wu
Chongqing University of Medical Science Clinical College: The First Affiliated Hospital of Chongqing Medical University

Jiewen Deng

Chongqing University of Medical Science Clinical College: The First Affiliated Hospital of Chongqing Medical University

Zhaohui He (geno_he@163.com)

Chongqing Medical University First Affiliated Hospital

Research

Keywords: Subarachnoid hemorrhage, Oligodendrocyte precursor cell differentiation disorder, Dexras1, White matter damage, glial cell activation

Posted Date: July 7th, 2021

DOI: https://doi.org/10.21203/rs.3.rs-672344/v1

Abstract

Background

White matter damage (WMD), different from the widely studied neuronal death, is also involved in neurological dysfunction after subarachnoid hemorrhage (SAH) although the specific mechanism is not yet known. Dexras1 (RASD1) has been reported to be involved in nervous system damage in autoimmune encephalitis and multiple sclerosis; however, there is no information on whether Dexras1 participates in WMD after SAH. We hypothesized that Dexras1 participates in oligodendrocyte precursor cell (OPC) differentiation in WMD after SAH.

Methods

Intracerebroventricular lentiviral administration was used to modulate Dexras1 levels to determine its functional influence on neurological injuries after SAH. Immunofluorescence, transmission electron microscopy, and Western blotting were used to investigate the effects of Dexras1 on demyelination, glial cell activation and differentiation of OPCs after SAH. Primary rat brain neurons were treated with oxyhemoglobin to elucidate the association between Dexras1 and cAMP-CREB.

Results

Dexras1 levels were significantly increased after SAH, accompanied by clear neurological deficits, glial cell activation, OPC differentiation disorders, and myelin injury. Dexras1 overexpression significantly worsened OPC dysdifferentiation and myelin injury after SAH, which were accompanied by increased glial cell activation and levels of inflammatory factors. In contrast, Dexras1 knockdown ameliorated demyelination, oligodendrocyte differentiation disorders, and glial cell activation. cAMP acted as an upstream agonist of CREB, with decreased TNF-α and IL-1β levels after SAH. However, the cAMP-CREB pathway was inhibited after Dexras1 overexpression.

Conclusion

Dexras1 induced oligodendrocyte dysdifferentiation after SAH and regulated glial cell activation through suppression of the cAMP-CREB pathway. This research highlights a novel direction for the improvement of neurological dysfunction after SAH.

1. Background

Aneurysmal subarachnoid hemorrhage(aSAH)is a critically severe neurosurgical disorder with extremely high mortality and disability[1, 2]. Despite intensive investigation of its pathological mechanism, this has not yet been fully elucidated. Previous research has shown that while neuronal death plays an important part in neurological dysfunction, it is not the only reason for neurological dysfunction after subarachnoid hemorrhage (SAH) [3, 4]. In recent years, white matter damage (WMD) after SAH has gradually become a research hotspot in neuroscience. Yusuke Egashira et.al[5]found that white matter fiber damage occurred

early after SAH, resulting in damage to both neuronal axons and oligodendrocytes (OLGs). Apart from neuronal death, nerve fiber demyelination associated with OLGs contributes significantly to permanent neurological injury [6, 7]. It is, therefore, possible that demyelination may occur after SAH and may play an important role in neurological dysfunction.

When the death of large numbers of OLGs results in myelin loss, a self-repairing process, remyelination, occurs[8]. In the central nervous system, OLGs act as myelin-forming cells. OLGs are differentiated from oligodendrocyte progenitor cells (OPCs), and only mature OLGs have the ability to form myelin[8]. Previous studies have shown that in myelin-related disorders, OPCs are often recruited around the lesion but cannot remyelinate until they differentiate into mature OLGs[9]. There are many factors affecting OLG differentiation and maturation, and the inflammatory response has been found to play a vital role among the many factors that cause WMD in demyelinated lesions[10]. Notably, Yiting Zhou et al.[11, 12] found that IL-1β and TNF-α can inhibit the aggregation, survival, and differentiation of OPCs, leading to dysfunctional remyelination and the aggravation of demyelination.

Dexamethasone-induced Ras-related protein 1 (Dexras1, also known as RASD1) is a brain tissue-rich guanylate-binding protein. Earlier reports have highlighted its influence in regulating circadian rhythms and tumor cell apoptosis[13]. Recently, it has been found that Dexras1 inhibits adenylyl cyclase activity in vitro, downregulating the cAMP-PKA-CREB signaling pathway[14]. It has also been found that blocking cAMP degradation and activation of cAMP-CREB pathway expression can significantly reduce the levels of TNF-α and the ILs, leading to a reduction in inflammation[15]. Therefore, we hypothesized that Dexras1 may promote inflammation by inhibiting the cAMP-CREB pathway.

Overall, we hypothesized that Dexras1 promotes inflammation through the cAMP-CREB pathway, and it is known that inflammation is one of the main pathological changes after SAH. Thus, we have good reason to believe that Dexras1 may play the same role in the inflammatory response that occurs after SAH. Therefore, this study explored the mechanism by which Dexras1 influences inflammation and the induction of WMD after SAH and provides basic support for further research on the treatment of SAH.

2. Materials And Methods

2. 1. Animals and study design

One hundred and fifty adult male Sprague–Dawley (SD) rats (280–350g) and 300 newborn (1-day-old) rat pups were obtained from the Animal Experiment Center of Chongqing Medical University. The rats were maintained in a specific pathogen-free environment under 12-hr light/dark cycles with regulated humidity and temperature. All research-related procedures received approval from the Animal Ethics and Use Committee of Chongqing Medical University. The rats were randomly assigned to the different groups: sham, SAH, SAH + LV-scramble, SAH + LV-Dexras1+, and SAH + LV-Dexras1-. The main endpoints were defined at 24 hr post-SAH.

2.2. SAH model constructed by endovascular perforation

The rat SAH model was established using a previously reported endovascular perforation method [16]. Briefly, the rats were anesthetized via intraperitoneal injection of pentobarbital (50 mg/kg), and the left carotid artery (CA) and its branches were exposed. Then, the distal end of the left external CA was sheared and reflexed to be in line with the left internal CA (ICA). A sharp 4 − 0 monofilament nylon suture was passed into the external CA and advanced through the ICA until resistance was encountered. The suture was then further advanced for roughly 3 mm to perforate the vessel bifurcation of the anterior and middle cerebral arteries. After puncturing for approximately 10 s, the filament was withdrawn. The sham group underwent identical procedures without the vascular puncture.

2.3. Culture of primary cortical neurons.

Primary cortical neurons were obtained from newborn SD rats as previously described[17]. Briefly, cortical tissues were extracted following newborn rat decapitation. The tissues were cut into small pieces and dispersed into cells (5 × 104 cells/mL), which were then grown in poly-D-lysine (Sigma, St. Louis, MO, USA)-coated (PDL-C) plates in Dulbecco's Modified Eagle Medium (DMEM) with 10% fetal bovine serum (FBS, Gibco, ThermoFisher Scientific, USA) for 4 h, following which the medium was replaced with neurobasal medium (Thermo Fisher Scientific) with 2% B27, 0.5 mM glutamine (ThermoFisher Scientific), 100 U/mL penicillin (P), and 100 µg/mL streptomycin (S) at 37°C with 5% CO2. The old medium was replaced with fresh medium every 3 days. Cells were used for experiments after culturing for 6 days.

2.4. Oxyhemoglobin incubated neural in vitro SAH model

To establish the neural in vitro SAH model, primary cortical neurons were treated with 10 µM oxyhemoglobin (OxyHb, O7109, Sigma, USA) in 1% DMSO for 24 h[18]. Control neurons were treated with 1% DMSO only. The treatment groups (SAH + LV-scramble, SAH + LV-Dexras1+, and SAH + LV-Dexras1-) were prepared with the OxyHb-exposed primary cortical cells for 24 h. In addition, an activator of the cAMP-CREB pathway, 8-Bromo-cAMP sodium salt (MCE, China, HY-12306), was also used to detect the effect of Dexras1 on cAMP-CREB pathway during SAH modeling. After these treatments, each measurement was conducted thrice to enhance the accuracy of the results.

2.5. Culture of OLN-93 rat oligodendroglia cells

OLN-93 rat oligodendroglia cells were purchased from Shanghai Binsui Biological Technology Co., Ltd. (China). The cells were cultured in DMEM with 10% heat-inactivated FBS, 100 U/ml P, and 100 µg/ml S. Cells were passaged once every three days and grown in an incubator at 37℃ with 5% CO2.

2.6. Differentiation of OLN-93 cells

The differentiation of OLN-93 cells into mature oligodendrocytes was performed as described by Van Meeteren et al[19]. OLN-93 cells were plated at 24 mm diameter dishes in DMEM with 0.5% FBS. After overnight (O/N) incubation, the medium was replaced with serum-free DMEM and incubated for three days, following which the medium was replaced again with fresh medium with 100 ng/ml IGF-I. Total protein was harvested for Western blot (WB) after six days. In addition,IGF-I-induced differentiated OLN-

93 cells seeded on PDL-C-coated 14 mm slides (Nest, China) before immunostaining with fluorescent maturation markers and comparative analysis against non-treated samples.

2.7. OLN-93 cell differentiation in co-culture with treated SAH neurons

Primary neurons were extracted as previously described and were seeded on 24-mm inserts with 0.4 μm pore size (Transwell-Clear Polyester Membrane; Corning Inc., USA) at a density of 0.5*106 cells with pre-suit corresponding medium, and incubated for six days. Then, IGF-I-mediated differentiated OLN-93 cells were seeded below the neurons. Samples from each of the treatment groups were collected for protein analysis after co-culture for three days. For immunofluorescence staining, IGF-I-differentiated cells were also plated on PDL-C-coated 14 mm slides and co-cultured for three days with each of the neuron treatment groups.

2.8. Drug and virus administration

2.8.1 Dexras1 up- and downregulated in vivo SAH model

In this experiment, overexpression and downregulation of the lentivirus Dexras1 sequence were used to verify Dexras1 function in the rat SAH model. The lateral ventricle injection method refers to the procedure introduced by HUANG JZ et al.[20]. Briefly, anesthetized rats were safely immobilized in a stereotaxic device (Stoelting, USA). Two to six microliters of the overexpression virus LV-Dexras1+ (109TU/mL), 2–6 μL of the knockdown virus LV-Dexras1 (109TU/mL), or control virus LV-Scramble (109TU/mL),purchased from Shanghai Genepharma Pharmaceutical Technology Co, Ltd., were slowly injected into the left lateral ventricle of each rat using a stereotactic frame (1.0 mm posterior to bregma, 1.5 mm lateral to midline, depth 3.5 mm under the surface of the skull) with a sterile 10-μL Hamilton syringe at a rate of 0.5 μL/min seven days before SAH modeling. A burr hole was also made in the sham rats but they did not receive intracerebroventricular injections. After injection and wound suturing, the rats were placed on an electric blanket for recovery with free access to food and water.

2.8.2 Virus-transfected in vitro SAH model

Lentiviral vectors carrying Dexras1 and GFP were generated by Genepharma (Shanghai, P.R. China). The lentivirus concentrations were 10^9 transducing units/mL and the sequences are shown in supplementary Table S1. Neurons were transfected with knockdown or overexpressing lentiviral vector carrying Dexras1 at an MOI (multiplicity of infection) of 80 [21]. An RNA duplex with random sequence was used as the negative control (NC). The transfection efficiency was 90%. Puromycin (2 μg/mL) was used to select transfected cells[22] which were then used for the experiments.

2.9. Evaluation of short-term neurobehavioral functions and SAH grade

The short-term neurobehavioral effects of treatments were assessed by blinded investigators at 24 h post-SAH according to the updated Garcia scale as previously described[23]. The modified Garcia scale includes six subtexts. The animals were given an overall score between 0 and 18 after summation of all scores. After evaluation of the neurological scores, the SAH severity was blindly assessed according to the previously described grading scale at the time of sacrifice[24, 25]. These scores also ranged from 0 to 18. Animals with a < 5 score were eliminated due to low SAH grade[26].

2.10. Morris Water Maze (MWM)

The MWM test was employed to assess the spatial learning ability and reference memory as previously described[23]. The cued water maze test was conducted before the SAH, and rats showing sensorimotor and/or motivational deficiencies affecting performance during the MWM test were not be included in further trials. The escape latency (EL) was measured on days 8 to 13 after SAH. During each acquisition test, rats were allowed 90 s to look for concealed platforms. If a rat was unable to find a platform within 90 s, it was directed there and allowed to rest on the platform for 20 s. On the 14th day, the platform was removed and the animals were observed for 90 s with a video recording system. The swimming pattern was assessed by an automatic image capture system to quantify distance, latency, and swimming speed. The number times of the rat crossed the platform and the time spent in the target quadrant were used for statistical analysis.

2.11. Western blot analysis

WB analysis was performed as previously described[23]. The left hemispheres of the rats were extracted and flash-frozen in liquid nitrogen before storing at -80℃ until further analysis. Cellular proteins were collected by cell scraping. The protein samples were then homogenized in RIPA lysis buffer and centrifuged for 15 min at 12 000 g at 4℃. Equal quantities of proteins (50μg) were then separated on 8%-15% SDS-PAGE gels and transferred to polyvinylidene fluoride (PVDF) membranes (0.2–0.4 μm). After blocking in 5% nonfat milk for 3 h at room temperature (RT), the membranes were incubated O/N at 4°C with individual primary antibodies as follows: anti-CNPase (1:250, Abcam, ab6319, USA), anti-Iba-1 (1:1000, Abcam, ab15690), anti-GFAP (1:1000, Abcam, ab10062), anti-myelin basic protein (MBP, 1:1000, Abcam, ab62631), anti-Dexras1 (1:1000, Abcam, ab78459), anti-CREB (1:1000, Cell Signaling, #9197, USA), anti-pCREB (1:500, Abcam, ab32096),anti-NG2 (1:500, Biorbyt, orb382135, UK) and anti-β-actin (1:1000, Cell Signaling, #4970), followed by corresponding secondary antibodies (1:5000, Biorbyt, orb572747/ orb557249) for 1 h at RT, and lastly, protein detection with a chemiluminescent reagent kit (ECL, Engreen Biosystem, New Zealand). Non-saturated bands were selected to perform densitometry quantification using Fusion (Fusion fx 7 Spectra, France) and the results are presented as a percentage, in comparison to the β-actin levels.

2.12. Immunofluorescence

Cells were collected from animals at 24 h after perforation for double-fluorescence staining, performed as previously described[23]. In brief, brain tissue specimens were perfused, dehydrated, and frozen at -80° C.

The samples were then sliced into 10 μm thick frozen sections, which were exposed O/N at 4°C to the individual primary antibodies as follows: anti-CNPase (1:50, Abcam, ab6319), anti-Iba-1 (1:50, Abcam, ab15690), anti-GFAP (1:50, Abcam, ab10062), anti-myelin basic protein (MBP, 1:50, Abcam, ab62631), anti-Dexras1 (1:50, Abcam, ab78459), anti-NG2 (1:50, Biorbyt, orb382135), anti-NEUN (1:50, Merck Millipore, USA). The appropriate secondary antibody (Proteintech, SA00003-1/ SA00009-2, Wuhan, China) was incubated with the sections at RT for 2 h, and the sections were observed and imaged using a fluorescence microscope (FV1200, Olympus, Japan).

2.13. Immunohistochemical study

Immunohistochemistry was done to assess NG2,CNPase, Dexras1, and GFAP immunoreactivities, as reported previously[27].The acquisition and preparation of animal tissue specimens was the same as for the immunofluorescence experiments except that the tissues were formalin-fixed, paraffin-embedded, and sliced after dehydration. The sections were then deparaffinized, rehydrated, and the endogenous peroxidase activity removed to repair the antigens. Nonspecific protein binding was eliminated by blocking with 5% goat serum for 1h and sections were then incubated O/N at 4°C with the following primary antibodies: anti-CNPase (1:50, Abcam, ab6319), anti-NG2 (1:50, Biorbyt, orb382135), anti-GFAP (1:50, Abcam, ab10062), and anti-myelin basic protein (MBP, 1:50, Abcam, ab62631). After three washes with PBS for 10 min,sections were exposed to the appropriate HRP-conjugated IgG (1:500 dilution; Santa Cruz Biotechnology, Inc., USA) for 60 min at 37℃. Finally, they were counterstained with hematoxylin, dehydrated in ethanol, and sealed with neutral balsam for microscopic observation.

2.14. RNA isolation and quantitative RT-PCR

Total RNA was isolated from cultured neurons with RNAiso Plus (TaKaRa, 9108, Dalian, China), following the kit operational guidelines. cDNA was prepared from mRNA with the PrimeScript® RT reagent Kit With gDNA Eraser, following the kit operational guidelines (TaKaRa, RR047A). The relative expression of the genes of interest was determined by quantitative PCR using SYBR® Premix Ex Taq™ II (TaKaRa, RR820A) and Premix Ex Taq RR390A (TaKaRa, RR390A). qPCR was performed with the BioMark HD Real-Time PCR System (Fluidigm). Thermal cyclic conditions were set to 2 min at 50°C, 10 min at 95°C, 30 sec at 95°C (denaturation), 3 0 sec at 58–60°C (annealing), and 30 sec at 72°C (extension) for 40 cycles. The overall volume per reaction was 10 μl, which consisted of 1 μl diluted cDNA (10 ng/uL), 5 μl Roche SyBR Green Master Mix, 0.5 μl double-distilled water, and 0.5 μl of relevant primers (10-mmol/L concentration). For primer sequences see following: Dexras1 ((Sense primer) 5'GGACGCTTACACCCCTACCAT3', (Anti-sense primer) 5' GGAAACGGATGATTGCCAGA 3'). The β-actin (Forward:5'-TGTCACCAACTGGGACGATA-3',Reverse:5'-GGGGTGTTGAAGGTCTCAAA-3')was used as an endogenous control gene. Data analysis was done with the Bio-Rad CFX Manager software.

2.15.Enzyme-linked immunosorbent assay (ELISA)

The culture medium was retrieved from all primary neuron cultures and the IL-1β and TNF-α levels measured using an ELISA assay (MULTISCIENCES, Hangzhou, China), following the kit operational

guidelines.

2.16. Transmission electron microscopy (TEM)

TEM was performed as described previously[28]. Twenty-four hours after SAH, the deeply anesthetized rats of each group were sacrificed by intracardial perfusion with 4% paraformaldehyde and 0.9 % saline. Then, the brain tissues were removed and post-fixed with 2% formaldehyde and 2% glutaraldehyde for 30 min. Next, the corpus callosum was minced into 1-mm3 pieces and maintained O/N at 4°C in the same fixation mixture, as described earlier. Following dehydration, samples were impregnated with epoxy resin and sectioned, before incubation with uranyl acetate and lead citrate. Finally, the electron micrographs were viewed using the Hitachi-7500 (Hitachi, Japan). Six random fields of view were imaged per section via TEM at a magnification of 12 000 x.

2.17. Statistical analysis

Data were expressed as means ± SD and analyzed with GraphPad Prism 8 (GraphPad Prism, USA). Unpaired t-tests or one-way ANOVAs were employed to analyze significance among thegroups. $P < 0.05$ was considered significant.

3. Results

3.1. Differentiation disorders of oligodendrocyte precursor cells and reduction of myelin after subarachnoid hemorrhage.

To investigate the differentiation disorders of oligodendrocyte precursor cells and myelin reduction after SAH, we successfully constructed an in vivo animal SAH model (Fig. 1A). The myelin marker protein MBP in the subcortex was detected by WB and immunofluorescence, and it was found that MBP expression was significantly reduced after SAH (Fig. 1B, C, G). These changes in MBP levels were further confirmed by immunohistochemical detection(Fig. 1H). The electron microscopy results showed significant loss and dissolution of myelin sheaths and even axonal injury after SAH(Fig. 1F).

There has been no relevant research investigating the differentiation of OPCs after SAH in the past. Therefore, immunofluorescence and other methods were used to verify OPC differentiation dysfunction after SAH. The immunofluorescence results showed that the levels of mature oligodendrocyte marker CNPase were decreased and the levels of oligodendrocyte precursor cell marker NG2 were increased after SAH(Fig. 1.G). WB results confirmed the decreased CNPase and increased NG2, showing gradual changes peaking at 24 h(Fig. 1B, D-E). The changes in CNPase and NG2 after SAH were also further confirmed by immunohistochemical detection(Fig. 1H).

3.2. Dexras1, TNF-α, and IL-1β levels, along with glial cell activation in SAH

There are no previous reports on the expression and localization of Dexras1 after SAH. Therefore, immunofluorescence was applied to detect the histological localization of Dexras1 in neurons, astrocytes, oligodendrocytes, and microglia after SAH. Specific markers were used to label neurons, astrocytes, oligodendrocytes, microglia, and to investigate their colocalization with Dexras1. Based on our data, Dexras1 was ubiquitous in neuronal cytoplasm in the cortex and hippocampus after SAH,with no obvious expression in microglia, astrocytes, and oligodendrocytes (Fig. 2D).

Next, the Dexras1, TNF-α, and IL-1β levels at different time intervals after SAH in vivo modeling were examined by WB and ELISA. The expression of Dexras1 after SAH was clearly increased in comparison with the sham group, and expression peaking at 24 h (Fig. 2A, B, $p < 0.01$). Relative to the controls, the expression of TNF-α (Fig. 2H $p < 0.001$) and IL-1β (Fig. 2I $p < 0.001$) were raised to different degrees. At the same time, the expression of GFAP(astrocyte marker)was also clearly enhanced after SAH(Fig. 2A, C). The immunofluorescence and immunohistochemical results showed that the numbers of astrocytes and microglia were clearly increased compared to the sham and that the astrocyte cell bodies of astrocytes were significantly thicker(Fig. 2E-G). These results indicate that SAH in rats leads to a significant increase in Dexras1 and produces inflammatory factors such as TNF-α and IL-1β.

3.3. Detection of glial cell activation, demyelination, and differentiation of oligodendrocyte precursor cells in vivo SAH model Dexras1 modulation

After the effective Dexras1 sequence for overexpression and knockdown was confirmed in the in vitro SAH model (Figure S1), it was injected into the lateral ventricle of SD rats. It was found that 6U lentivirus Dexras1 + and Dexras1- could significantly increase or decrease the expression of Dexras1 after SAH (Fig. 3A-B). At the same time, the rat myelin marker (MBP) was further reduced in the SAH + LV- Dexras1 + rats($p < 0.05$,Fig. 3A, C),relative to the SAH + LV-Scramble rats. After down-regulation by LV-Dexras1-, relative to the SAH + LV-Scramble rats, the expression of MBP in SAH + LV-Dexras1- rats was significantly increased ($p < 0.05$, Fig. 3A.C).

In addition, the myelin marker protein MBP in the rat brain cortex detected by immunofluorescence showed that MBP expression was further reduced and the texture of the myelin sheath became weaker in the SAH + LV-Dexras1 + group (Fig. 3.J); After down-regulation of LV-Dexras1, relative to the SAH + LV-Scramble rats, MBP expression was markedly increased and the myelin texture was clearer in the SAH + LV-Dexras1- group (Fig. 3.J).

The changes in myelin sheath in the corpus callosum were also examined by electron microscopy. The results showed that myelin sheaths in the SAH + LV-Dexras1 + group were further reduced, even broken, and the axon separation became more noticeable (Fig. 3H); However, relative to the SAH + LV-Scramble rats, the myelin sheath swelling and axon myelin sheath separation were clearly alleviated in the SAH + LV-Dexras1- group (Fig. 3H).

Next, marker proteins for astrocyte and microglial activation were detected by WB. It was found that GFAP and Iba1 were significantly increased after SAH ($P < 0.05$, Fig. 3A, D-E). After Dexras1 up-regulation and

down-regulation, the expression of GFAP,Iba1,TNF-α, and IL-1β in SAH + LV-Dexras1 + rats were elevated, relative to the SAH + LV-Scramble rats ($P < 0.01$, Fig. 3A, D-E, L-M), while the expression of GFAP,Iba1,TNF-α, and IL-1β in SAH + LV-Dexras1- group was significantly decreased ($P < 0.05$, Fig. 3A, D-E, L-M).

At the same time, the astrocyte and microglial activation marker proteins GFAP and Iba1 in the rat brain cortices were detected by immunofluorescence. After Dexras1 up-regulation and down-regulation in SD rats, the astrocyte and microglial activation in the SAH + LV-Dexras1 + group was further increased relative to the SAH + LV-Scramble rats (Fig. 3J, K), while, in contrast to the up-regulation, the astrocyte and microglial activation in the SAH + LV-Dexras1- group was further reduced relative to the SAH + LV-Scramble rats (Fig. 3J, K).

To further verify whether Dexras1 was involved in the differentiation of OPCs after SAH, the changes in CNPase and NG2 levels after SAH in rats after Dexras1 lentivirus intervention were detected by WB and immunofluorescence. The results showed that CNPase levels in the SAH + LV-Dexras1 + group were further decreased ($P < 0.05$, Fig. 3A, G), while there was a significant increase in NG2 ($P < 0.05$, Fig. 3A, F), relative to the SAH + LV-Scramble rats. Moreover, there was recovery of CNPase in the SAH + LV-Dexras1- rats ($P < 0.05$, Fig. 3A, G) while NG2 was significantly decreased ($P < 0.05$, Fig. 3A, F). The immunofluorescence results also showed that the expression of CNPase, a marker protein of mature oligodendrocytes, was reduced in the SAH + LV-Dexras1 + rats in conjunction with significantly disordered myelin texture. Meanwhile, the marker of oligodendrocyte precursor cells, NG2, was further elevated in the SAH + LV-Dexras1 + rats (Fig. 3I). However, relative to the SAH + LV-Scramble rats, CNPase levels in the SAH + LV-Dexras1- rats were markedly elevated, accompanied by the restoration of myelin structure while NG2 was significantly reduced (Fig. 3I).

3. 4. Dexras1 can significantly aggravate neurological deficits after SAH modeling in SD rats.

SAH can significantly aggravate neurological deficits. The neurological scores of the SAH rats at 24 h (24 h = 10.40 ± 0.55, n = 5, Fig. 4A, $p < 0.05$) were drastically reduced, relative to the sham rats (18.00 ± 0.00). The scores of the SAH + LV-Dexras1 + rats(8.20 ± 0.84)were lower than those of the SAH + LV-Scramble rats(10.60 ± 0.55)($p < 0.05$,Fig. 4A). However, the scores of the SAH + LV-Dexras1- rats (14.20 + 0.23) were remarkably enhanced, relative to the SAH + LV-Scramble rats(10.60 ± 0.55)($p < 0.05$,Fig. 4A). These results indicate that Dexras1 can significantly aggravate neurological dysfunction in rats post-SAH.

In addition, the water content of brain tissue is also an important indicator for evaluating brain damage post-SAH. Relative to the sham rats, the brain tissue water content increased drastically after SAH at 24 h ($P < 0.05$, Fig. 4B). After up or down-regulating Dexras1 in SD rats, relative to the SAH + LV-Scramble rats, the brain edema in the SAH + LV-Dexras1 + rats was markedly elevated ($P < 0.05$, Fig. 4B) while was significantly reduced in the SAH + LV-Dexras1-rats ($P < 0.05$, Fig. 4B).

The escape latencies (EL) of all five groups of rats through acquisition training (5 days) are illustrated in Fig. 4G. All rats exhibited obvious enhancements in the EL after 5 days of training [$F(4,76)6.063$, $p = 0.002$, repeated measures ANCOVA], suggesting that they had memory of the escape platform (EP).

Repeated measures ANCOVA suggested no relationship between training days and groups [F(4,76)329.454, p = 0.003]. Hence, all the animals had learned the task adequately. Moreover, the EL of the SAH rats was remarkably longer, relative to the sham rats (F(4, 76)14.78,P < 0.0001,Fig. 4G). In addition, the SAH + LV-Dexras1 + group showed clearly aggravated deficiencies (F(4, 76)2.955,p = 0.0252,Fig. 4G) while the SAH + LV-Dexras1-group did not(F(4, 76)3.732,P = 0.0079, Fig. 4G).

After five days of acquisition training, the rats mastered the search of the EP. To evaluate memory, on day 6, the rats were placed in the pool for 90 s without an EP, recording the number of times across the platform, as well as the time and distance of staying within the target quadrant where the EP is located. Multiple comparisons using one-way analysis of variance indicated that the residence time and number of crossings of the SAH rats were markedly less than those of the sham rats(p□0.01,Fig. 4C-F. The SAH + LV-Dexras1 + rats showed further reductions relative to the SAH + LV-Scramble rats(p□0.01,Fig. 4C-F). However, the SAH + LV-Dexras1-group increased the residence time, distance, and the number of crossings of the platform after SAH(p□0.01, Fig. 4C, F).

3.5. Disordered oligodendrocyte precursor cell differentiation occurred in vitro cultured neurons after SAH with or without Dextras1 intervention

Following Van Meeteren et al.'s report that IGF-1 can promote the differentiation of OLN-93 oligodendrocytes into mature oligodendrocytes[19], we further tested the differentiation of oligodendrocyte precursor cells in in vitro culture after SAH and in co-culture with IGF-treated cells using Transwell assays. The results showed that the in vitro neuronal SAH model can inhibit the differentiation and maturation of OLN-93 oligodendrocyte precursor cells induced by IGF-1 (Fig. 5A). WB also revealed that NG2 expression was markedly elevated and CNPase was clearly reduced post-SAH in IGF-1-co-cultured cells (P < 0.05,Fig. 5B-C).

Additionally, to determine whether Dexras1 regulates oligodendrocyte precursor cell differentiation in the in vitro-cultured neurons after SAH, Transwell assays were used to co-culture up- and down-regulated Dexras1 neuronal SAH model cells with IGF-treated OLN-93 cells. The immunofluorescence data revealed that CNPase levels were reduced in the SAH + LV-Dexras1 + rats, and NG2 was further increased (Fig. 5D). Relative to the SAH + LV-Scramble rats, CNPase in the SAH + LV-Dexras1- rats was markedly elevated, while NG2 was significantly reduced (Fig. 5D). The WB results also showed that, relative to the SAH + LV-Scramble rats, the CNPase in the SAH + LV-Dexras1 + rats was further decreased (P < 0.05, Fig. 5E-F), while NG2 was further significantly increased (P < 0.05, Fig. 5E-F). However, the expression of CNPase in the SAH + LV-Dexras1- group recovered (P < 0.05, Fig. 5E-F) while NG2 was significantly decreased (P < 0.05, Fig. 5E-F).

3.6. Dexras1 may inhibit the differentiation of oligodendrocyte precursor cells through the cAMP-CREB pathway

After up-regulation and down-regulation of Dexras1, it was found that the expression of IL-1β and TNF-α in the SAH + LV-Dexras1 + rats was markedly elevated relative to the SAH + LV-Scramble rats ($P < 0.05$, Fig. 6A ,B, D), accompanied by significant decreases in CREB and pCREB proteins ($P < 0.05$, Fig. 6A, C). In addition, the expression of IL-1β and TNF-α in the SAH + LV-Dexras1- rats were significantly lower, relative to the SAH + LV-Scramble rats ($P < 0.05$, Fig. 6A, B, D), accompanied by significant increases in the CREB and pCREB proteins ($P < 0.05$, Fig. 6A, C).

To further investigate whether Dexras1 promotes TNF-α and IL-1β through the cAMP-CREB pathway, we first examined the effects of 8-Bromo-cAMP sodium salt, a specific agonist of the cAMP-CREB pathway, on the changes in IL-1β and TNF-α after SAH. Similar to previous experimental results, it was found that CREB was significantly reduced in SAH, and IL-1β and TNF-a were significantly increased(Fig. 6A-D). In contrast, CREB was significantly elevated after 8-Bromo-cAMP sodium salt intervention, and the IL-1β and TNF-α levels were drastically decreased($P < 0.05$,Fig. 6F-H). These results indicate that 8-Bromo-cAMP sodium salt activates the expression of the cAMP-CREB pathway.

Next, after overexpressing Dexras1, the 8-Bromo-cAMP sodium salt was used to investigate the effect of Dexras1 on the cAMP-CREB pathway. At the same time, after knocking down Dexras1, we further verified the effect of Dexras1 on the cAMP pathway by using the 8-Bromo-cAMP sodium salt. Using WB and immunofluorescence, we found that the levels of CREB and pCREB in the Dexras1 overexpression + 8-Bromo-cAMP group were significantly lower than in the SAH + 8-Bromo-cAMP group, accompanied by a reduction in CNPase($P < 0.05$,Fig. 6I-J). However, the levels of CREB and pCREB in the Dexras1 knockdown + 8-Bromo-cAMP group were clearly higher than in the SAH + 8-Bromo-cAMP group accompanied by an increase in CNPase($P < 0.05$,Fig. 6I-J). Further investigation revealed that TNF-α,IL-1β, and NG2 in the Dexras1 overexpression + 8-Bromo-cAMP-treated cells were markedly elevated, relative to the SAH + 8-Bromo-cAMP-treated cells($P < 0.05$,Fig. 6E, J-K). However, TNF-α,IL-1β, and NG2 in the Dexras1 knockdown + 8mbp-treated cells were considerably reduced in the SAH + 8-Bromo-cAMP-treated cells ($P < 0.05$,Fig. 6E, J-K). These results suggest that Dexras1 may promote inflammation by inhibiting the cAMP-CREB pathway, eventually leading to differentiation dysfunction in OPCs.

4. Discussion

SAH is classified as a severe neurosurgical illness and SAH patients tend to experience severe neurological dysfunction. Previous studies on SAH have mainly focused on the gray matter represented by neurons while less attention has been paid to the brain white matter with abundant nerve fibers. YEO et al[30]found, in a study of 22 SAH cases, that patients can develop corticospinal tract (CST) damage after seven weeks of bleeding, leading to the weakening of motor function in patients with subarachnoid hemorrhage. Egashira Y et al [31]also found that oligodendrocytes and neuronal axons can be damaged early after SAH in mice. These research results indicate that WMD after SAH may be an important pathological contributor to neurological dysfunction and the main cause of poor prognosis for patients. However, there have been few studies on WMD after SAH.

WMD is common in many demyelinating diseases, and its characteristic pathological changes include OLG death, remyelination disorder, and axon damage. Among these many pathological changes, the demyelination caused by the death of OLGs and disorders of remyelination have particular pathological significance, which can destroy the integrity of axons as they lose the protective effect of the myelin sheath,thus affecting the conduction of nerve impulses and axonal transport, which are important causes of brain dysfunction[32]. Previous studies have also confirmed the presence of demyelination in neurological diseases such as multiple sclerosis and autoimmune encephalitis, and demyelination is known to significantly aggravate neurological dysfunction related to both motor and cognitive behavior[33–35]. It has also been discovered that there may be demyelination changes after SAH but this has not been studied or confirmed in depth[6]. Therefore, to clarify whether there is demyelination after SAH, we investigated myelin changes in the corpus callosum, cortex, and other parts of the rat brain after SAH by immunofluorescence and electron microscopy. It was found that there were clear sparse,swollen, and loosened laminae in the myelin sheaths, with clearly disordered and reduced myelin texture, even leading to separation from the axons. In addition, the neurobehavioral scores and water maze results in this study suggest that SD rats not only have early neurological dysfunction after SAH, but also show long-term behavioral, memory, and learning dysfunction. These results demonstrate conclusively that the myelin sheath is lost and damaged after SAH, which is among the primary manifestations of WMD after SAH, and can cause marked early neurological dysfunction, even leaving long-term neurological dysfunction. This also prompts us to not only pay attention to neurons, but also strengthen research on nerve fiber damage when we conduct research on SAH in the future.

The myelin sheath of the central nervous system is a membrane that wraps around the axons of neurons and is composed of mature OLGs. It has the function of insulating and protecting axons and can significantly increase the conduction speed of nerve impulses[32]. When demyelination occurs in adults due to various diseases, OPCs can differentiate into mature OLGs and re-wrap the axons for remyelination, repairing the conduction of nerve impulses. This process is often limited by various physiological and pathological factors[8]. Previous studies have confirmed that in demyelination-related diseases, OPCs often accumulate around the lesion, but cannot further differentiate and mature, and eventually form Olgs with remyelination ability[9, 29, 36]. The above studies indicate that dysfunctional OPC differentiation is one of the main causes of demyelination in diseases such as multiple sclerosis and autoimmune encephalitis. However, there is no relevant research focusing on the role of oligodendrocyte differentiation disorder in neurological dysfunction post-SAH. Therefore, we employed WB and immunofluorescence to assess changes in the marker proteins of oligodendrocyte precursors and mature cells after SAH in vivo and in vitro and observed that the markers and numbers of mature oligodendrocytes were markedly low following SAH, while the expression of oligodendrocyte precursor cells increased significantly. These results suggest that there is a significant deficit in oligodendrocyte precursor cell differentiation after SAH, and this is among the main reasons for demyelination post-SAH. In addition, cerebral edema, as the most common pathological process following SAH, may also modulate demyelination by increasing local tissue pressure and stretching myelinated fiber bundles, which is similar to the findings of previous studies[37].

There are various pathological mechanisms that affect the differentiation and maturation of OPCs and inflammatory factors are known to play a pivotal role in them. Yiting Zhou et al. [11]found that IL-1β can inhibit the accumulation of OPCs in a model of ischemic hypoperfusion injury caused by unilateral CA occlusion, leading to remyelination disorders and aggravating demyelination. In addition, studies have found that TNF-α can inhibit the survival and differentiation of OPCs in autoimmune encephalitis and spinal cord injury, leading to demyelination[12, 38]. The above studies show that inflammatory factors can significantly inhibit the differentiation and survival of oligodendrocyte precursor cells and participate in neurological dysfunction in CNS-related diseases. Appropriately, the inflammatory response also plays an extremely important role after subarachnoid hemorrhage, and is mainly characterized by increased levels of inflammatory factors such as TNF-a and IL-1β, cellular edema, and inflammatory cell infiltration[39]. Furthermore,prior reports have also suggested that WMD may be related to inflammation, oligodendrocyte ferroptosis and apoptosis[40, 41]. To sum up, we urgently want to determine whether the inflammatory response after SAH may also lead to WMD through the differentiation of oligodendrocyte precursor cells. Gratifyingly, our experimental results also found that IL-1β and TNF-α are significantly increased after SAH, accompanied by significant obstacles to oligodendrocyte precursor cell differentiation. These results strongly indicate that the significant increases in TNF-α, IL-1β, and other inflammatory factors after SAH may be one of the main reasons for these obstacles to the differentiation of oligodendrocyte precursor cells after SAH and may ultimately participate in post-SAH demyelination and WMD. Therefore, reducing the inflammatory response after SAH may be of great significance for improving the differentiation of oligodendrocyte precursor cells and improving neurological function after SAH.

Dexras1 is a small G protein activated by nitric oxide (NO), which is produced in activated microglia/macrophages or neurons[42]. The previous research on Dexras1 mainly focused on regulating circadian rhythms, tumor cell apoptosis, and other aspects[43, 44]. However, Khan et al [45]found that,after Dexras1 knockdown,there was an improvement to myelin damage in experimental optic neuritis, suggesting that Dexras1 may modulate myelin damage through some unknown mechanism. However,it is unclear whether Dexras1 is also involved in the WMD characterized by myelin damage after SAH.

Our study found that Dexras1 levels increased significantly after SAH. At the same time, this and previous studies by our group also found that SAH can significantly increase TNF-α, IL-1β, and other inflammatory factors[46]. In this study, the SAH model was constructed after up-regulation and down-regulation of Dexras1, and found that TNF-α and IL-1β increased and decreased in a coordinated manner in response to Dexras1 overexpression and knockdown, respectively, accompanied by respective reductions and increases in the levels of the myelin basic protein MBP; corresponding changes were also observed in the myelin sheaths with immunofluorescence and electron microscopy. At the same time, our research also found that Dexras1 can cause a marked activation of astrocytes and microglia. These changes are similar to the myelin sheath changes caused by WMD after cerebral ischemia[47]. It can be seen that these results all confirm that Dexras1 is involved in WMD after SAH, and the mechanism may be related to the promotion of inflammation by Dexras1. This is consistent with the conclusion of Song et al. [48] that the glial cell-mediated inflammatory response is involved in WMD in the ischemic stroke model.

Multiple reports have suggested that Dexras1 can suppress adenylate cyclase activity and aggravate oxidative stress[14, 42], while other scholars have found that inflammation after SAH is closely related to oxidative stress[49]. The findings of these studies suggest that Dexras1 may participate in inflammatory response regulation after SAH by affecting the adenylate cyclase pathway and oxidative stress. The present study further confirmed that both SAH and Dexras1 overexpression can lead to a significant decrease in CREB, and Dexras1 upregulation can further block the cAMP pathway activation by 8-Bromo-cAMP, and that the inflammatory factors TNF-α and IL-1β are significantly up-regulated after Dexras1 overexpression in the in vitro SAH model. At the same time, the differentiation of oligodendrocyte precursor cells was also significantly inhibited by Dexras1 in the in vitro SAH model. Therefore, based on this evidence, Dexras1 may promote inflammation by suppressing the activity of adenylate cyclase and aggravating oxidative stress after SAH, and may then inhibit the differentiation of oligodendrocyte precursor cells, leading to demyelination and WMD after SAH.

5. Conclusion

In summary, our study is the first to confirm the existence of demyelination after SAH, and to investigate the hypothesis that Dexras1 mediates the inflammatory response by inhibiting the cAMP-CREB pathway, which, in turn, leads to the differentiation disorder of oligodendrocyte precursor cells after SAH. These research results may offer novel therapeutic targets for the prevention and treatment of WMD after SAH, especially the loss of myelin sheath, and provide an experimental basis for the formulation of new treatment strategies for SAH. Nevertheless, the pathological mechanisms of WMD are complex and diverse. Our research is just a drop in the ocean among many mechanisms. In the future, we not only need to explore the many manifestations of white matter injury after SAH but we still need more research to determine other potential contributions of Dexras1 to WMD after SAH. This will prompt clinicians to pay more attention to the role of myelin loss after SAH and is expected to provide research support for clinical work.

Abbreviations

SAH: Subarachnoid hemorrhage; WMD: White matter damage; Dexras1(Rasd1): Dexamethasone-induced Ras-related protein1; OPC: oligodendrocyte precursor cells; CREB: cAMP-response element binding protein; cAMP: Cyclic adenosine monophosphate; MBP: myelin basic protein; cDNA: complementary DNA; PBS: Phosphate buffer saline; LV: Lentivirus; OLGs: oligodendrocytes; PKA: protein kinase A; Iba-1: Ionized calcium-binding adapter molecule 1; IL-1β: Interleukin-1 beta; RT-qPCR: Real-time quantitative polymerase chain reaction; TNF-α: Tumor necrosis factor alpha; CNPase: cyclic nucleotide 3'phosphohydrolase; NG2: neural/glial antigen 2; OLN-93: rat oligodendroglia cells; GFAP: glial fibrillary acidic protein; IGF-1: insulin-like growth factor-I.

Declarations

Competing interests

The authors declare that they have no competing interests

Acknowledgments

The authors thank the National Natural Science Foundation of China and Natural Science Foundation Project of Chongqing Science and Technology Commission for their financial support, and also thank the Central Laboratory of the First Affiliated Hospital of Chongqing Medical University for providing experimental sites and related equipment support.

Funding

The study was supported by research grants from the National Natural Science Foundation of China (NO. 81870927), and Natural Science Foundation Project of Chongqing Science and Technology Commission (NO. cstc2019jcyj-msxmX0239).

Availability of data and materials

The datasets generated and/or analyzed during the current study are available from the corresponding author on reasonable request.

Authors' contributions

Yuanjun Xin designed the research, performed the experiments, collected and analyzed the data, and drafted the manuscript. Zhaohui He handled the funding, provided useful advice on the design of this study, and supervised the experimental. Hongxia Zhang provided initial project idea on the design of this study. Jun Zhao, Xiang Xiang, Fu Ming Liang and Wenqiao Fu performed part of the experiments. Jie Chen,Yidan Liang, Hao Huang, Xintong Wu and Jiewen Deng worked on and revised the manuscript. All the authors read and approved the final manuscript.

Consent for publication

Not applicative.

Ethics approval

All animal experiments were conducted according to a protocol approved by the Animal Ethics and Use Committee of Chongqing Medical University (Permit No.SCXK (Chongqing) 2007–0001).

References

1. Lawton MT, Vates GE. Subarachnoid Hemorrhage. N Engl J Med. 2017;377(3):257-66.

2. Macdonald RL, Schweizer TA. Spontaneous subarachnoid haemorrhage. Lancet 2017; 389(10069):655-66.

3. Cahill J, Calvert JW, Zhang JH. Mechanisms of early brain injury after subarachnoid hemorrhage. J Cereb Blood Flow Metab. 2006;26(11):1341-53.

4. Chen S, Feng H, Sherchan P, Klebe D, Zhao G, Sun X, et al. Controversies and evolving new mechanisms in subarachnoid hemorrhage. Prog Neurobiol. 2014;115:64-91.

5. Egashira Y, Zhao H, Hua Y, Keep RF, Xi G. White Matter Injury After Subarachnoid Hemorrhage: Role of Blood-Brain Barrier Disruption and Matrix Metalloproteinase-9. Stroke 2015;46(10):2909-15.

6. Simard JM, Tosun C, Ivanova S, Kurland DB, Hong C, Radecki L, et al. Heparin reduces neuroinflammation and transsynaptic neuronal apoptosis in a model of subarachnoid hemorrhage. Transl Stroke Res. 2012;3(Suppl 1):155-65.

7. Wu Y, Peng J, Pang J, Sun X, Jiang Y. Potential mechanisms of white matter injury in the acute phase of experimental subarachnoid haemorrhage. Brain 2017;140(6):e36.

8. Kuhlmann T, Miron V, Cui Q, Wegner C, Antel J, Brück W. Differentiation block of oligodendroglial progenitor cells as a cause for remyelination failure in chronic multiple sclerosis. Brain 2008;131(Pt 7):1749-58.

9. Kotter MR, Stadelmann C, Hartung HP. Enhancing remyelination in disease–can we wrap it up?. Brain 2011;134(Pt 7):1882-900.

10. Stephenson J, Nutma E, van der Valk P, Amor S. Inflammation in CNS neurodegenerative diseases. Immunology 2018;154(2):204-19.

11. Zhou Y, Zhang J, Wang L, Chen Y, Wan Y, He Y, et al. Interleukin-1beta impedes oligodendrocyte progenitor cell recruitment and white matter repair following chronic cerebral hypoperfusion. Brain Behav Immun. 2017;60:93-105.

12. Su Z, Yuan Y, Chen J, Zhu Y, Qiu Y, Zhu F, et al. Reactive astrocytes inhibit the survival and differentiation of oligodendrocyte precursor cells by secreted TNF-alpha. J Neurotrauma. 2011;28(6):1089-100.

13. Fang M, Jaffrey SR, Sawa A, Ye K, Luo X, Snyder SH. Dexras1: a G protein specifically coupled to neuronal nitric oxide synthase via CAPON. Neuron 2000;28(1):183-93.

14. Greenwood MP, Greenwood M, Mecawi AS, Antunes-Rodrigues J, Paton JF, Murphy D. Rasd1, a small G protein with a big role in the hypothalamic response to neuronal activation. Mol Brain. 2016;9:1.

15. Atkins CM, Oliva AA Jr, Alonso OF, Pearse DD, Bramlett HM, Dietrich WD. Modulation of the cAMP signaling pathway after traumatic brain injury. Exp Neurol. 2007; 208(1):145-58.

16. Duris K, Manaenko A, Suzuki H, Rolland WB, Krafft PR, Zhang JH. α7 Nicotinic acetylcholine receptor agonist PNU-282987 attenuates early brain injury in a perforation model of subarachnoid hemorrhage in rats. Stroke 2011;42(12):3530-6.

17. Su F, Yang S, Wang H, Qiao Z, Zhao H, Qu Z. CIRBP Ameliorates Neuronal Amyloid Toxicity via Antioxidative and Antiapoptotic Pathways in Primary Cortical Neurons. Oxid Med Cell longev. 2020;2020:2786139.

18. Zhang T, Wu P, Zhang JH, Li Y, Xu S, Wang C, et al. Docosahexaenoic Acid Alleviates Oxidative Stress-Based Apoptosis Via Improving Mitochondrial Dynamics in Early Brain Injury After Subarachnoid Hemorrhage. Cell Mol Neurobiol. 2018;38(7):1413-23.

19. Meeteren ME, Koetsier MA, Dijkstra CD, van Tol EA. Markers for OLN-93 oligodendroglia differentiation. Brain Res Dev Brain Res. 2005;156(1):78-86.

20. Huang JZ, Ren Y, Jiang Y, Shen SY, Ding J, Hua F. GluR1 protects hypoxic ischemic brain damage via activating Akt signaling pathway in neonatal rats. Eur Rev Med Pharmacol Sci. 2018;22(24):8857-65.

21. Morgan RA, Unti MJ, Aleshe B, Brown D, Osborne KS, Koziol C, et al.Improved Titer and Gene Transfer by Lentiviral Vectors Using Novel, Small β-Globin Locus Control Region Elements. Mol Ther. 2020;28(1):328-40.

22. Lou G, Chen L, Xia C, Wang W, Qi J, Li A, et al. MiR-199a-modified exosomes from adipose tissue-derived mesenchymal stem cells improve hepatocellular carcinoma chemosensitivity through mTOR pathway. J Exp Clin Cancer Res. 2020;39(1):4.

23. Mo J, Enkhjargal B, Travis ZD, Zhou K, Wu P, Zhang G, et al. AVE 0991 attenuates oxidative stress and neuronal apoptosis via Mas/PKA/CREB/UCP-2 pathway after subarachnoid hemorrhage in rats. Redox Biol. 2019; 20:75-86.

24. Mielke D, Bleuel K, Stadelmann C, Rohde V, Malinova V. The ESAS-score: A histological severity grading system of subarachnoid hemorrhage using the modified double hemorrhage model in rats. PloS one 2020;15(2):e0227349.

25. Suzuki H, Hasegawa Y, Chen W, Kanamaru K, Zhang JH. Recombinant osteopontin in cerebral vasospasm after subarachnoid hemorrhage. Ann Neurol. 2010;68(5):650-60.

26. Sugawara T, Ayer R, Jadhav V, Zhang JH. A new grading system evaluating bleeding scale in filament perforation subarachnoid hemorrhage rat model. J Neurosci Methods 2008;167(2):327-34. DOI:10.1016/j.jneumeth.2007.08.004

27. Wang Z, Wu L, You W, Ji C, Chen G. Melatonin alleviates secondary brain damage and neurobehavioral dysfunction after experimental subarachnoid hemorrhage: possible involvement of TLR4-mediated inflammatory pathway. J Pineal Res. 2013;55(4):399-408.

28. Yang C, Li T, Xue H, Wang L, Deng L, Xie Y, et al. Inhibition of Necroptosis Rescues SAH-Induced Synaptic Impairments in Hippocampus via CREB-BDNF Pathway. Front Neurosci. 2018;12:990.

29. Sim FJ, Zhao C, Penderis J, Franklin RJ. The age-related decrease in CNS remyelination efficiency is attributable to an impairment of both oligodendrocyte progenitor recruitment and differentiation. J Neurosci. 2002;22(7):2451-9.

30. Yeo SS, Choi BY, Chang CH, Kim SH, Jung YJ, Jang SH. Evidence of corticospinal tract injury at midbrain in patients with subarachnoid hemorrhage. Stroke 2012;43(8):2239-41.

31. Egashira Y, Hua Y, Keep RF, Xi G. Acute white matter injury after experimental subarachnoid hemorrhage: potential role of lipocalin 2. Stroke 2014;45(7):2141-3.

32. Wang Y, Li B, Li Z, Huang S, Wang J, Sun R. Improvement of hypoxia-ischemia-induced white matter injury in immature rat brain by ethyl pyruvate. Neurochem Res. 2013;38(4):742-52.

33. Desai RA, Davies AL, Del Rossi N, Tachrount M, Dyson A, Gustavson B, et al. Nimodipine Reduces Dysfunction and Demyelination in Models of Multiple Sclerosis. Ann Neurol. 2020.

34. Kamboj A, Lu P, Cossoy MB, Stobart JL, Dolhun BA, Kauppinen TM, et al. Poly(ADP-ribose) polymerase 2 contributes to neuroinflammation and neurological dysfunction in mouse experimental autoimmune encephalomyelitis. J Neuroinflamm. 2013;10:49.

35. Till C, Noguera A, Verhey LH, O'Mahony J, Yeh EA, Mah JK, et al. Cognitive and Behavioral Functioning in Childhood Acquired Demyelinating Syndromes. J Int Neuropsychol Soc. 2016;22(10):1050-60.

36. Miron VE, Kuhlmann T, Antel JP. Cells of the oligodendroglial lineage, myelination, and remyelination. Biochim Biophy Acta 2011;1812(2):184-93.

37. Barz H, Schreiber A, Barz U. Demyelinating diseases as a result of cerebral edema?. Med Hypotheses 2017;104:10-4.

38. Valentin-Torres A, Savarin C, Barnett J, Bergmann CC. Blockade of sustained tumor necrosis factor in a transgenic model of progressive autoimmune encephalomyelitis limits oligodendrocyte apoptosis and promotes oligodendrocyte maturation. J Neuroinflamm. 2018;15(1):121.

39. Okada T, Suzuki H. Mediators involved in brain injury following subarachnoid hemorrhage. Histol Histopathol. 2020;18208.

40. Zanno AE, Romer MA, Fox L, Golden T, Jaeckle-Santos L, Simmons RA, et al. Reducing Th2 inflammation through neutralizing IL-4 antibody rescues myelination in IUGR rat brain. J Neurodev Disord. 2019;11(1):34.

41. Leonetti C, Macrez R, Pruvost M, Hommet Y, Bronsard J, Fournier A, et al. Tissue-type plasminogen activator exerts EGF-like chemokinetic effects on oligodendrocytes in white matter (re)myelination. Mol Neuro. 2017;12(1):20.

42. Bouchard-Cannon P, Lowden C, Trinh D, Cheng HM. Dexras1 is a homeostatic regulator of exercise-dependent proliferation and cell survival in the hippocampal neurogenic niche. Sci Rep. 2018;8(1):5294.

43. Cheng HY, Obrietan K. Dexras1: shaping the responsiveness of the circadian clock. Sem Cell Dev Biol. 2006;17(3):345-51.

44. Thapliyal A, Verma R, Kumar N. Small G Proteins Dexras1 and RHES and Their Role in Pathophysiological Processes. Int J cell Biol. 2014;2014:308535.

45. Khan RS, Baumann B, Dine K, Song Y, Dunaief JL, Kim SF, et al. Dexras1 Deletion and Iron Chelation Promote Neuroprotection in Experimental Optic Neuritis. Sci Rep. 2019;9(1):11664.

46. Lee S, Min Kim S, Dotimas J, Li L, Feener EP, Baldus S, et al. Thioredoxin-interacting protein links endoplasmic reticulum stress to inflammatory brain injury and apoptosis after subarachnoid haemorrhage. J Neuroinflamm. 2017;14(1):104.

47. Zhao Y, Wang H, Chen W, Chen L, Liu D, Wang X, et al. Melatonin attenuates white matter damage after focal brain ischemia in rats by regulating the TLR4/NF-kappaB pathway. Brain Res Bulle. 2019;150:168-78.

48. Song S, Wang S, Pigott VM, Jiang T, Foley LM, Mishra A, et al. Selective role of Na /H exchanger in Cx3cr1 microglial activation, white matter demyelination, and post-stroke function recovery. Glia 2018;66(11):2279-98.

49. Zhuang K, Zuo YC, Sherchan P, Wang JK, Yan XX, Liu F. Hydrogen Inhalation Attenuates Oxidative Stress Related Endothelial Cells Injury After Subarachnoid Hemorrhage in Rats. Front Neurosci. 2019;13:1441.

Figures

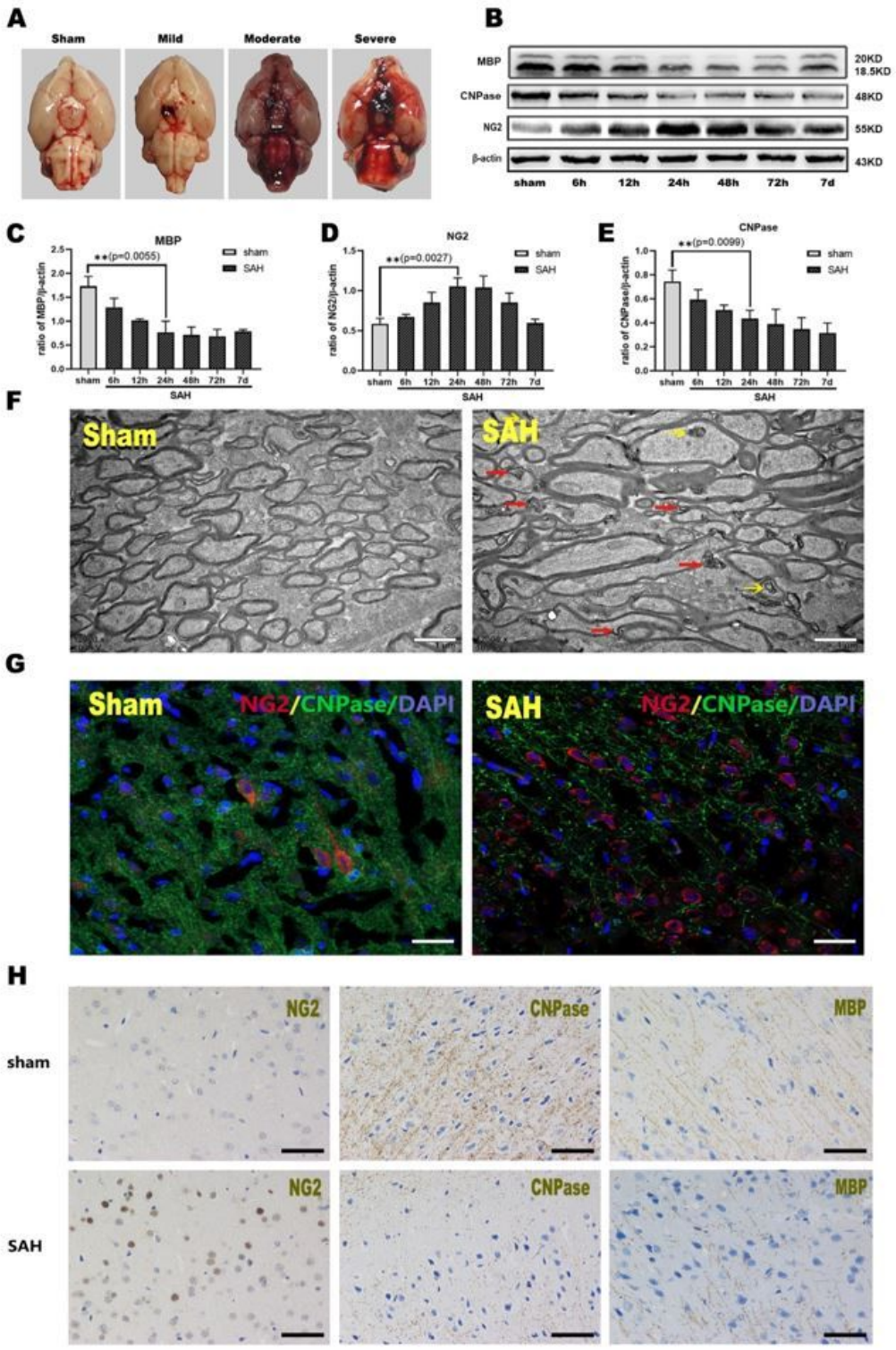

Figure 1

(A). Differential severity of the endovascular perforation SAH model; (B). Typical Western blot of MBP, CNPase, and NG2; (C-E). Protein quantification for MBP and associated proteins, analyzed by Fusion (fx 7 Spectra, Vilber, France). Results are presented as percentages in relation to β-actin levels. $p<0.05$ vs. Sham. (F). Loss of myelin sheaths 24 hours after SAH evaluated by transmission electron microscopy, showing significant loss and fracture damage red arrow) and clearly disordered axonal structure and

damage (yellow arrow); scale bar=1 μm (n=5). (G). Histological fluorescence staining for CNPase and NG2 in cortices of the sham group and 24 h after SAH. NG2 (labels oligodendrocyte precursor cells, red); DAPI (the nucleus, blue), CNPase(labels mature oligodendrocyte cells, green);(n=3). (H). Immunohistochemical staining for CNPase, MBP, and NG2 in cortices of the sham group and 24h after SAH. Compared with the control group, NG2 (labels oligodendrocyte precursor cells,brown)are clearly increased, CNPase(labels mature oligodendrocyte cells, brown), and MBP indicate significantly disordered and reduced myelin texture (C-D, n=3). detected by histochemical microscopy, Olympus, Japan). Scale bars: e= 25μm.

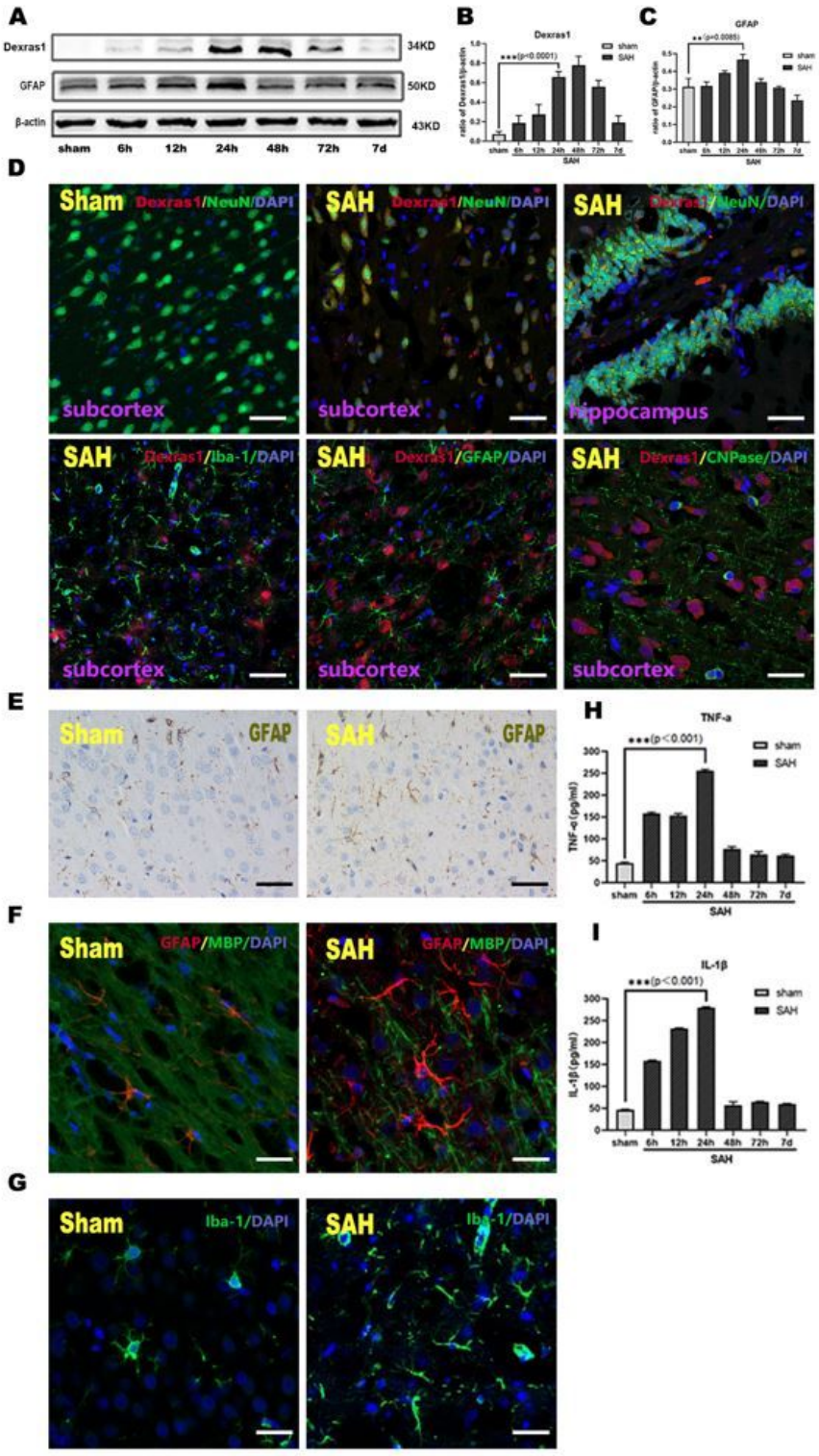

Figure 2

(A). Representative Western blot of Dexras1 and GFAP; (B-C). Protein quantification of Dexras1 and GFAP, analyzed by Fusion (fx 7 Spectra, Vilber, France). Results are presented as percentages in relation to β-actin levels. $p<0.05$ vs. Sham. (D). Typical histological immunofluorescence staining showing co-localization of Dexras1 in neurons, astrocytes, microglia, and oligodendrocytes in the cortex and hippocampus 24 h post-SAH. Dexras1(red) was detected with NeuN (neurons, green), Iba-1 (microglia,

green), GFAP (astrocytes, green), and CNPase (oligodendroglias, green) in the cortex and hippocampus after SAH, DAPI (nucleus, blue), (n=3); scale bars: e= 25 μm. (E). Immunohistochemical staining for GFAP in the cortex of the sham group and 24 h after SAH. Compared with the control group, GFAP (brown, n=3)is clearly increased, detected by histochemical microscopy, (Olympus, Japan). Scale bars: e=25 μm. (F). Histological fluorescent staining for GFAP and MBP in the cortex of the sham group and 24 h after SAH. (GFAP- labels astrocytes,red), DAPI (nucleus, blue),MBP(labels myelin, green)(n=3)). Scale bars: e=25 μm. (G). Histological fluorescent staining of Iba-1 in the cortex of the sham group and 24 h after SAH. (Iba-1 labels microglia,green)and DAPI (nucleus, blue). Scale bars: e= 25 μm. (H-I). Representative ELISA of TNF-α and IL-1β;

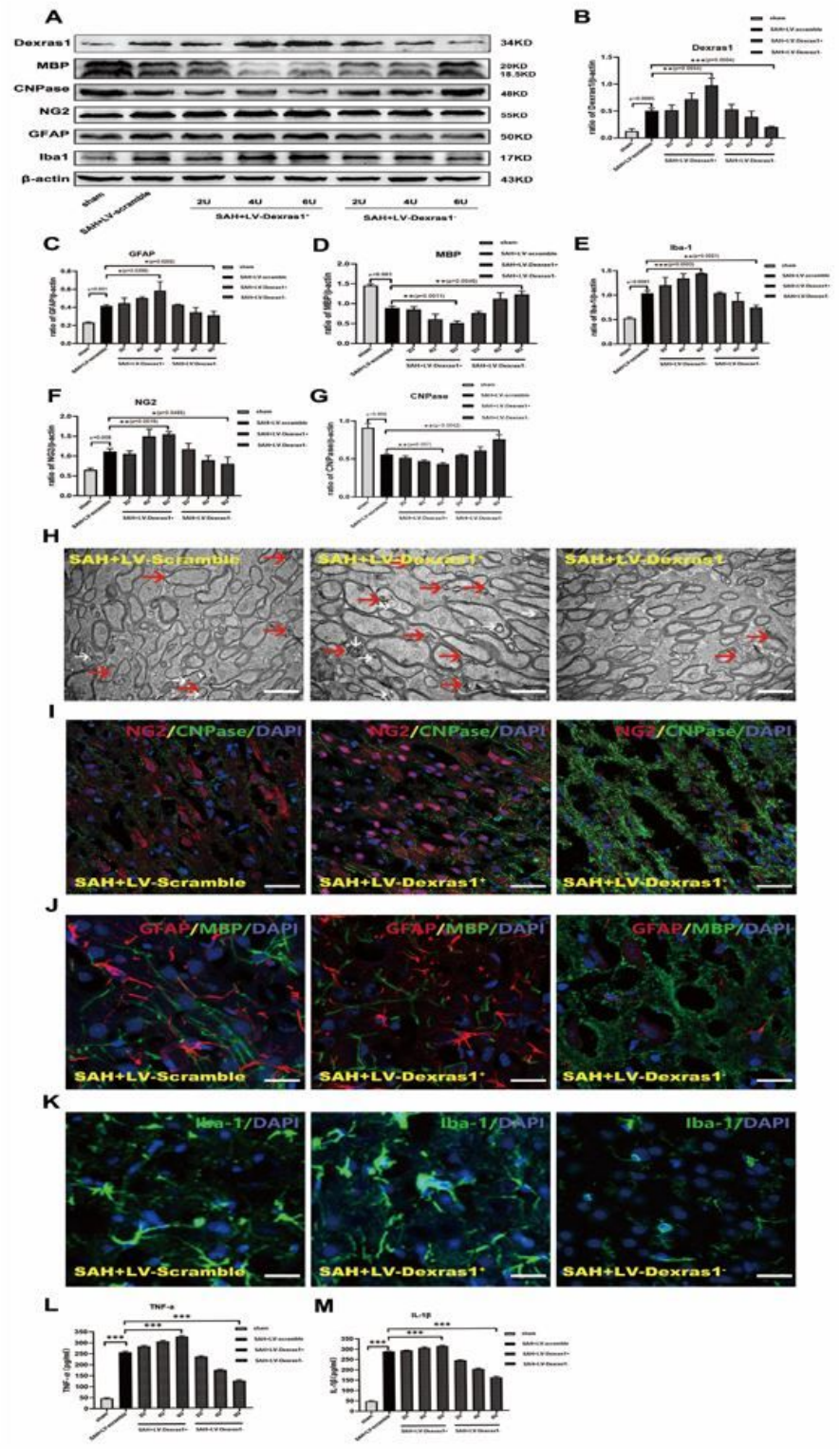

Figure 3

(A). Representative Western blot of Dexras1, MBP, CNPase, NG2, GFAP, and Iba1 expression in each group (sham, SAH + LV-scramble, SAH +LV-Dexras1+ and the SAH +LV-Dexras1- with different concentrations of virus). (B-G). Western blot semi-quantitative analysis. Results are expressed as percentages in relation to β-actin levels. (* p <0.05, ** p <0.01, *** p <0.001). (H). the loss of myelin sheaths in SAH+LV-Scramble, SAH +LV-Dexras1+and SAH +LV-Dexras1- rats was evaluated by transmission electron microscopy.

demyelination (black arrow) and axon separation (yellow arrow). Scale bar, 1 μm (n=5 for electron microscopy analysis). (I). Histological fluorescent staining for CNPase and NG2 in the cortex of SAH+LV-Scramble, SAH +LV-Dexras1+and SAH +LV-Dexras1- rats. NG2(labels oligodendrocyte precursor cells,red), DAPI (nucleus, blue),CNPase(labels mature oligodendrocyte cells, green). Scale bar =25μm. (J). Histological fluorescence staining of GFAP and MBP in the cortex of the SAH+LV-Scramble group, SAH +LV-Dexras1+, and SAH +LV-Dexras1- group. GFAP(labels astrocytes,red),DAPI (nucleus, blue) ,MBP(labels myelin, green)(n=3), detected by fluorescence microscopy. Scale bars: e=25μm. (K). Histological fluorescent staining for Iba-1 in the cortex of the SAH+LV-Scramble group, SAH+LV-Dexras1+, and SAH +LV-Dexras1- group. Iba-1(labels microglia,green), DAPI (nucleus, blue). detected by fluorescence microscopy. Scale bars: e=25μm. (L-M). Representative ELISA of TNF-α and IL-1β

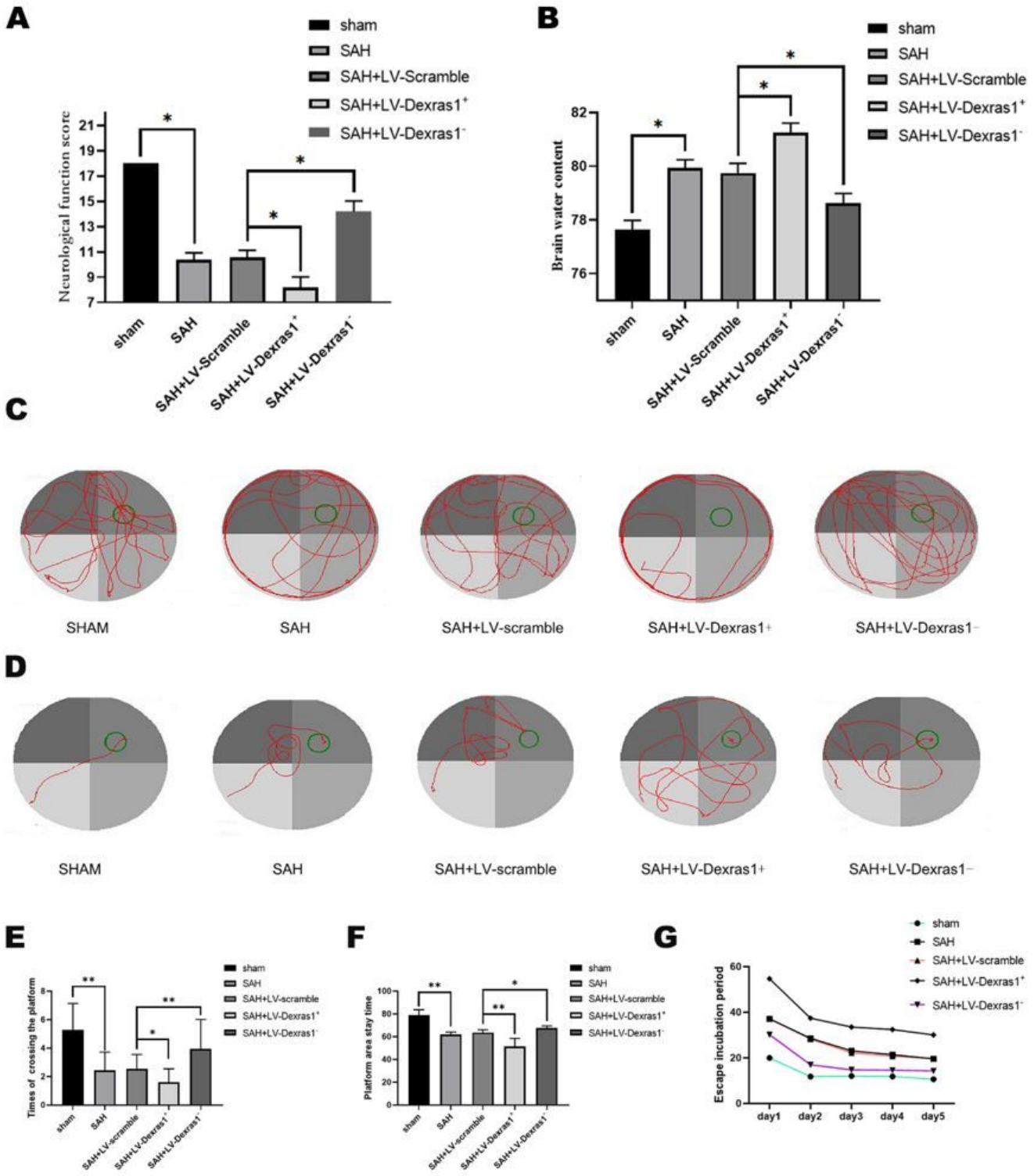

Figure 4

(A). Analysis of neurological deficits at 24 hours in each group; *p<0.05 sham vs SAH rats, *p<0.05,SAH +LV-Dexras1+ vs SAH+LV-Scramble rats, *p<0.05 SAH +LV-Dexras1- vs SAH+LV-Scramble rats; (B). Evaluation of water in brain tissue in each group after SAH, *p<0.05 sham vs SAH rats, *p<0.05 SAH +LV-Dexras1+ vs SAH+LV-Scramble rats, *p<0.05 SAH +LV-Dexras1- vs SAH+LV-Scramble rats; (C). Day 6 track displays of all rats; recording was done for 90 s after training platform removal; (D). Representative

images of the shortest path of each group to the platform during the acquisition trials in the MWM examination; (E). The times of each group crossed the platform; recording was done for 90 s after training platform removal; (F). Analysis of the percentage of time rats remained in the target quadrant during the spatial exploratory test; (G). Seven days post-SAH, rats were allowed 90 s to search for the hidden platform; each acquisition trial was part of 4 trials, one per day, for 5 days. Data represent mean±SD, n=5, *p<0.05 sham vs SAH rats, *p<0.05 SAH+LV-Dexras1+ vs SAH+LV-Scramble rats, *p<0.05 SAH+LV-Dexras1- vs SAH+LV-Scramble rats;

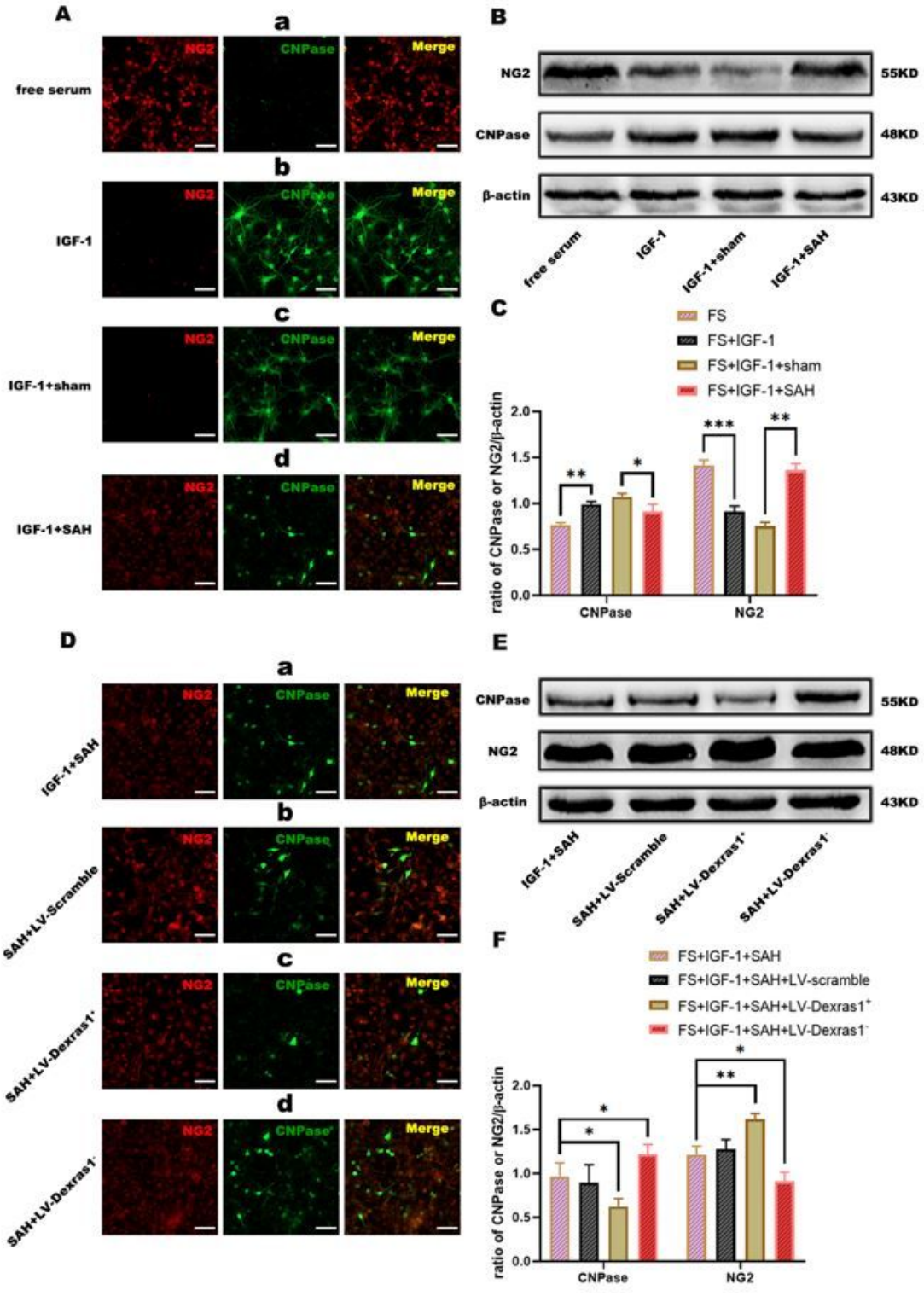

Figure 5

(A). Immunofluorescence detection of oligodendrocyte precursor cell differentiation after in vitro subarachnoid hemorrhage, Serum-free culture of oligodendrocyte cell line(a),IGF-1 and serum-free medium promote oligodendrocyte cell line differentiation (b),Co-culture of sham group neurons and oligodendrocyte cell line treated with IGF-1(c),Co-culture of SAH group neurons and oligodendrocyte cell line treated with IGF-1(d). OPCs (NG2, red), OLGs (CNPase, green). Scale bars: e= 25 μm. (B). Protein expression of NG2 and CNPase after 24 h in vitro co-culture with oligodendrocyte cell treated with IGF-1. (C). NG2 and CNPase protein quantification via Fusion (fx 7 Spectra, Vilber, France). Data are given as percentages relative to the β-actin level. $p<0.05$ IGF-1+SAH vs. IGF-1+Sham rats. (D). Immunofluorescence detection of oligodendrocyte precursor cell line differentiation in vitro IGF-1 and serum-free medium with SAH, SAH+LV-Scramble, SAH+LV-Dexras1+, and SAH+LV-Dexras1- rats. Co-culture of SAH group neurons and oligodendrocyte cells treated with IGF-1(a),Co-culture of SAH+LV-Scramble group neurons and oligodendrocyte cells treated with IGF-1(b),Co-culture of SAH+LV-Dexras1+ group neurons and oligodendrocyte cell line treated with IGF-1(c),Co-culture of SAH+LV-Dexras1- group neurons and oligodendrocyte cells treated with IGF-1(d). OPCs (NG2, red), OLGs (CNPase, green),Scale bars: e=25 μm. (E). Protein expression of NG2 and CNPase after 24 h in vitro co-culture of each group with oligodendrocyte cells treated with IGF-1. (F). NG2 and CNPase protein quantification via Fusion (fx 7 Spectra, Vilber, France. Data in percentages relative to the β-actin level. (* $p<0.05$, ** $p<0.01$).

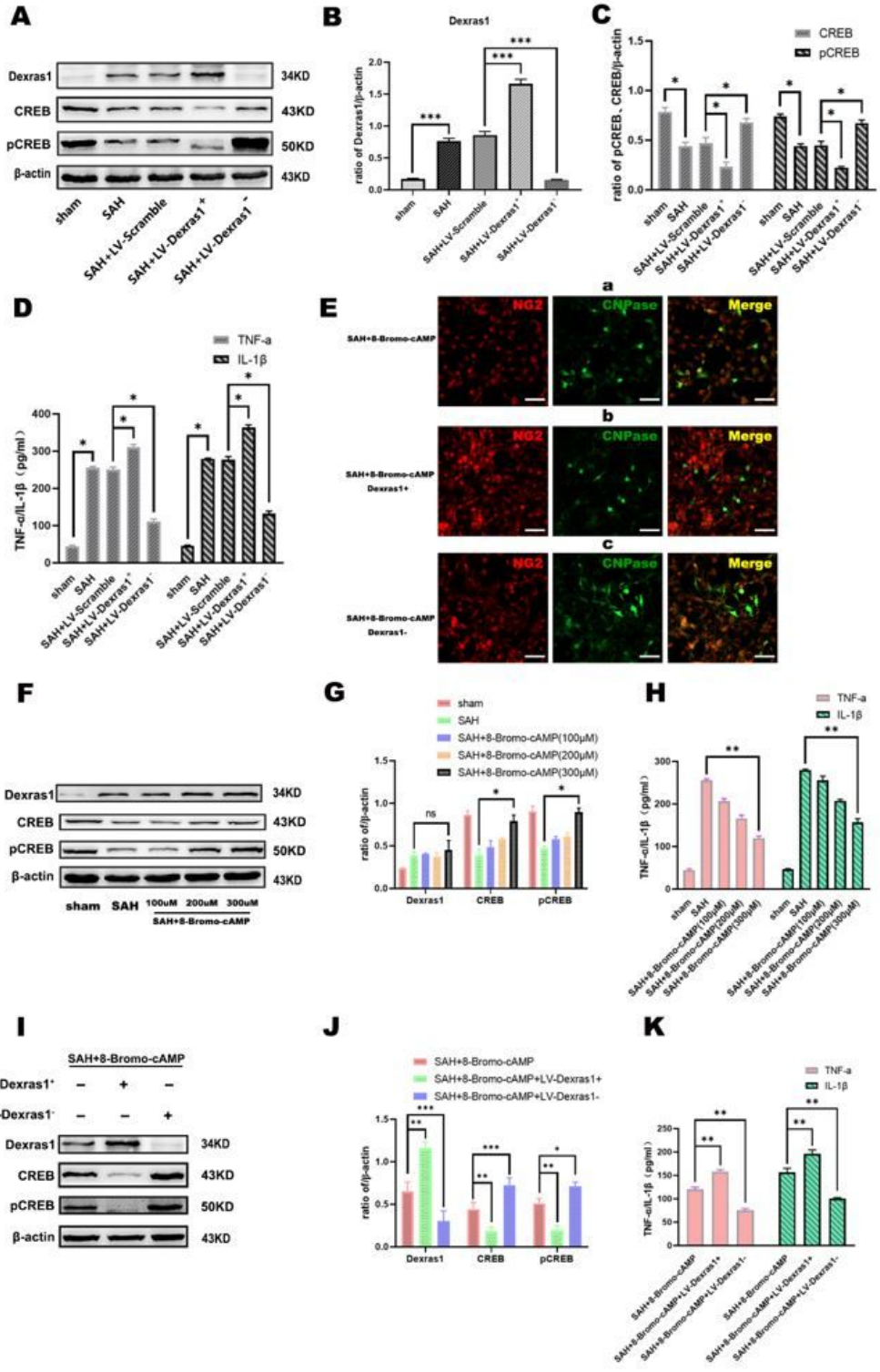

Figure 6

(A). Western blot detection Dexras1, CREB, and pCREB protein expression after intervention with LV-Dexras1+ or LV-Dexras1-;(B-C).Western blot analysis (* p <0.05, ** p <0.01); (D). ELISA to detect the expression of IL-1β and TNF-α. (E). Immunofluorescence detection of oligodendrocyte precursor cell line differentiation after in vitro subarachnoid hemorrhage in each group, co-culture of SAH+8-Bromo-cAMP group neurons and oligodendrocyte cells treated with IGF-1(a),Co-culture of SAH+8BMP+Dexras1+group

neurons and oligodendrocyte cells treated with IGF-1(b), Co-culture of SAH+8-Bromo-cAMP+Dexras1-group neurons and oligodendrocyte cells treated with IGF-1(c), OPCs (NG2, red), OLGs (CNPase, green),Scale bars: e= 25 μm. (F). Representative Western blot of Dexras1, CREB, and pCREB expression after subarachnoid hemorrhage in vitro with activation by different 8-Bromo-cAMP sodium salts; (G) Western blot semi-quantitative analysis of Dexras1, CREB, and pCREB. Results are percentages relative to β-actin levels. (* $p < 0.05$, ** $p < 0.01$); (H). ELISA to detect IL-1β and TNF-α levels. (I). A typical Western blot of Dexras1, CREB, and pCREB after 8-Bromo-cAMP sodium salt treatment combined with Dexras1 overexpression and knockdown after subarachnoid hemorrhage in vitro. (J) Western blot semi-quantitative analysis of Dexras1, CREB, and pCRE. Results are percentages relative to β-actin levels. (* $p < 0.05$, ** $p < 0.01$) (K). ELISA to detect IL-1β and TNF-α levels.

Supplementary Files

This is a list of supplementary files associated with this preprint. Click to download.

- Additionaldocuments.docx